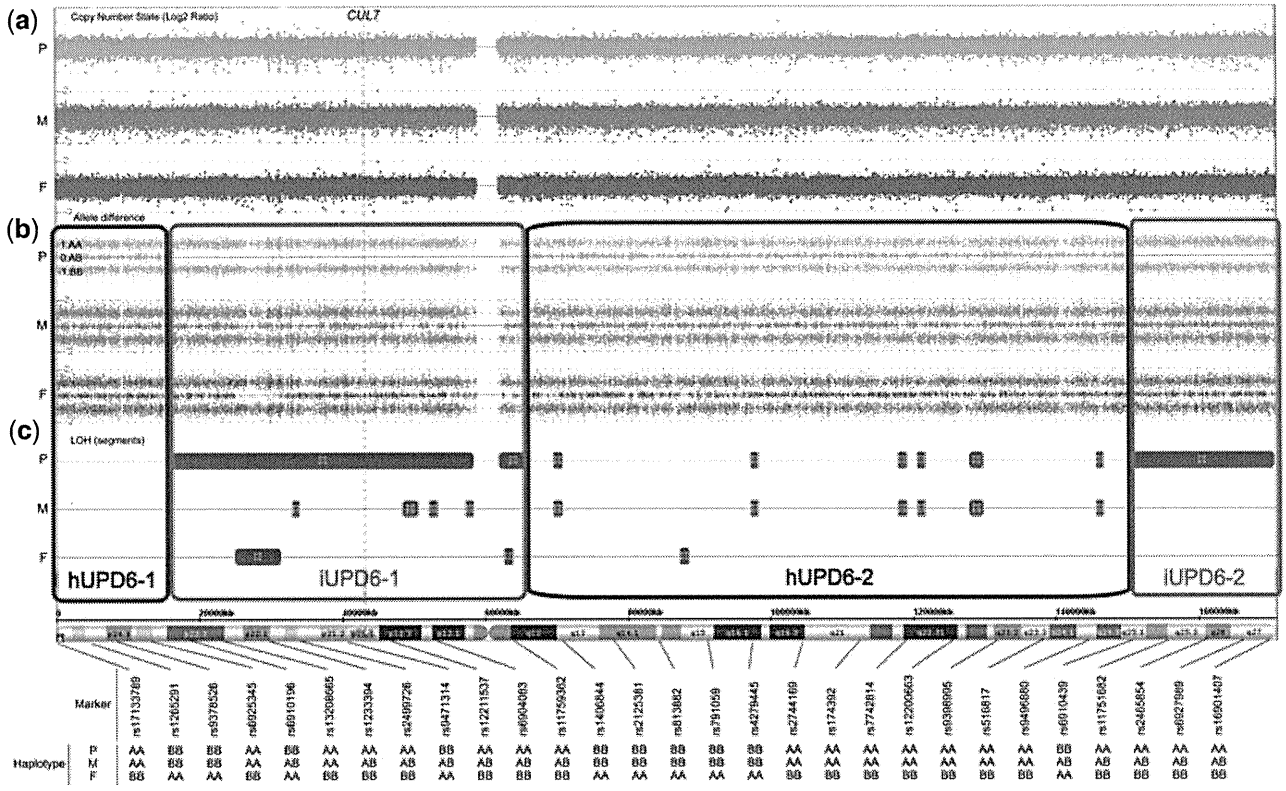

Fig. 2. SNP6.0 data. (**a**) Plots of the SNP6.0 data displayed in ChAS 1.0.1 showing the log2 ratio plot of copy number state, allele difference plot, and loss of heterozygosity (LOH) segment (purple box) (P, patient; M, mother; and F, father). (**b**) The allele difference graph represents the genotypes for each individual single nucleotide polymorphism (SNP). Dots with a value of 1, −1, and 0 represent SNPs with AA, BB, and AB genotypes, respectively. A vertical dashed line indicates the *CUL7* locus. (**c**) The LOH segment plot indicates nine LOH regions on chromosome 6. iUPD6-1 and iUPD6-2 denote the regions of uniparental isodisomy (red box). hUPD6-1 and hUPD6-2 denote the regions of uniparental heterodisomy (blue box). The genotypes on chromosome 6 indicate maternal heterodisomy or isodisomy in the affected offspring [only the uniparental disomy (UPD) markers are displayed].

Table 1. Examination of SNPs from a patient/father/mother trio[a]

			hUPD6-1	iUPD6-1	hUPD6-2	iUPD6-2
Genotype of trio (patient/father/mother)	iUPD	AA/BB/AB	0	534	0	318
		BB/AA/AB	0	576	3	304
	iUPD or hUPD	AA/BB/AA	178	543	605	272
		BB/AA/BB	196	506	563	262
Share genotype (patient/mother)	iUPD or hUPD	AA/AA	2,812	5,897	9,716	3,009
		BB/BB	2,799	5,785	9,557	2,919
	hUPD	AB/AB	1,699	19	6,384	12
		Total of share genotype	7,310	11,701	25,657	5,940
		Share genotype rate (%)	99.82	78.20	99.89	73.31
		Total SNP probe	7,323	14,963	25,684	8,103
		Start SNP	rs4959515	rs9370869	rs9354209	rs9384189
		Start position	110,391	16,290,223	65,799,990	150,518,012
		End SNP	rs9477050	rs9453156	rs7765984	rs6931065
		End position	16,287,166	65,796,893	150,517,779	170,759,956
		Size (bp)	16,176,776	49,506,671	84,717,790	20,241,945
		Cytoband	p25.3-p22.3	p22.3-q12	q12-q25.1	q25.1-q27

hUPD, uniparental heterodisomy; iUPD, uniparental isodisomy; iUPD or hUPD, UPD could not be defined as isodisomy or heterodisomy; SNP, single nucleotide polymorphism.

[a]Each row contains information on each matUPD6 inheritance block identified by trio haplotype analysis.

both the X chromosome and chromosome 6 showed maternal iUPD. This case also was notable for IUGR and growth retardation at 8 months of age (15). The fifth case was a fetus with IUGR at 29 weeks of pregnancy from a 45-year-old patient. The case was ascertained as trisomy 6 mosaicism in cultured chorionic villi but disomy in amniocytes; analysis of DNA markers in amniocytes and parental samples revealed mat-iUPD6 in disomy cells (16). The sixth case was a male infant with molybdenum cofactor deficiency who showed developmental delay. SNP analysis with the trio revealed that at least 6p21.1-6p24.3 were mat-iUPD6, but not another region were remain unclear (17). The seventh case was a patient with cleft lip and palate, and showed a complete maternal hUPD on chromosome 6 (mat-hUPD6). This case had no notable IUGR in the serial ultrasound examination (18). Taken together, IUGR and growth retardation were found in the cases with mat-iUPD6 (12, 13, 15–17), while these were not found in cases with mat-hUPD6 (14, 18). The IUGR and growth retardation in cases of mat-iUPD6 may be the result of homozygosity of chromosome 6. On the basis of these reports, no clear maternal imprinting effect of chromosome 6 can be established; however, recently, a complete gain of methylation phenotype at insulin-like growth factor 2 receptor was shown in patients with growth restriction (19).

The patient with homozygous mutation in *CUL7* and matUPD6 had clinical features compatible with 3M syndrome. However, the patient displayed certain features that have not been previously reported among patients with *CUL7* mutations such as mild mental retardation, inguinal hernia, hydrocele testis, and mild ventricular enlargement (7, 8, 20). Mild mental retardation is an especially characteristic phenotype in our case because most patients with 3M syndrome have normal intelligence. It is difficult to determine whether matUPD6 had a significant role in the development of certain feature in our case.

Here we report a case of 3M syndrome with a homozygous mutation that resulted from maternal iUPD, including the *CUL7* gene. Although complete paternal or maternal UPD for chromosome 6 has previously been reported, this is the first report of a patient with 3M syndrome who has a mixture of mat-hUPD6 and mat-iUPD6 regions. Our results emphasize that UPD should be considered possible mechanism for developing the autosomal recessive disorders including 3M syndrome.

Acknowledgements

We are grateful to the patient and his parents for their participation in this research. We also thank Ms Miho Ooga and Ms Chisa Hayashida for technical assistance. K.-I. Y. was supported in part by Grants-in-Aid for Scientific Research from the Ministry of Health, Labour and Welfare, and in part by the Takeda Scientific Foundation and the Naito Foundation.

References

1. Winter RM, Baraitser M, Grant DB, Preece MA, Hall CM. The 3-M syndrome. J Med Genet 1984: 21: 124–128.
2. Feldmann M, Gilgenkrantz S, Parisot S, Zarini G, Marchal C. 3M dwarfism: a study of two further sibs. J Med Genet 1989: 26 (9): 583–585.
3. García-Cruz D, Cantú JM. Heterozygous expression in 3-M slender-boned nanism. Hum Genet 1979: 52: 221–226.
4. Mueller RF, Buckler J, Arthur R et al. The 3-M syndrome: risk of intracerebral aneurysm? J Med Genet 1992: 29: 425–427.
5. Le Merrer M, Brauner R, Maroteaux P. Dwarfism with gloomy face: a new syndrome with features of 3-M syndrome. J Med Genet 1991: 28: 186–191.
6. Spranger J, Opitz JM, Nourmand A. A new familial intrauterine growth retardation syndrome the "3-M syndrome". Eur J Pediatr 1976: 123: 115–124.
7. Huber C, Dias-Santagata D, Glaser A et al. Identification of mutations in *CUL7* in 3-M syndrome. Nat Genet 2005: 37: 1119–1124.
8. Huber C, Delezoide AL, Guimiot F et al. A large-scale mutation search reveals genetic heterogeneity in 3M syndrome. Eur J Hum Genet 2009: 17: 395–400.
9. Hanson D, Murray PG, Sud A et al. The primordial growth disorder 3-M syndrome connects ubiquitination to the cytoskeletal adaptor *OBSL1*. Am J Hum Genet 2009: 84: 801–806.
10. Huber C, Fradin M, Edouard T et al. OBSL1 mutations in 3-M syndrome are associated with a modulation of IGFBP2 and IGFBP5 expression levels. Hum Mutat 2010: 31: 20–26.
11. Engel E. A new genetic concept: uniparental disomy and its potential effect, isodisomy. Am J Med Genet 1980: 6: 137–143.
12. van den Berg-Loonen EM, Savelkoul P, van Hooff H, van Eede P, Riesewijk A, Geraedts J. Uniparental maternal disomy 6 in a renal transplant patient. Hum Immunol 1996: 45: 46–51.
13. Spiro RP, Christian SL, Ledbetter DH et al. Intrauterine growth retardation associated with maternal uniparental disomy for chromosome 6 unmasked by congenital adrenal hyperplasia. Pediatr Res 1999: 46: 510–513.
14. Cockwell AE, Baker SJ, Connarty M, Moore IE, Crolla JA. Mosaic trisomy 6 and maternal uniparental disomy 6 in a 23-week gestation fetus with atrioventricular septal defect. Am J Med Genet A 2006: 140: 624–627.
15. Parker EA, Hovanes K, Germak J, Porter F, Merke DP. Maternal 21-hydroxylase deficiency and uniparental isodisomy of chromosome 6 and X results in a child with 21-hydroxylase deficiency and Klinefelter syndrome. Am J Med Genet A 2006: 140: 2236–2240.
16. Haag M, Beischel L, Rokeach J et al. First prenatal detection of maternal uniparental disomy (UPD) of chromosome 6 and 'rescue' of trisomy 6 [abstract]. *Abstracts of the 57th Annual Meeting of the ASHG 2007*; Abstract no 2428.
17. Gümüş H, Ghesquiere S, Per H et al. Maternal uniparental isodisomy is responsible for serious molybdenum cofactor deficiency. Dev Med Child Neurol 2010: 52 (9): 868–872.

18. Salahshourifar I, Halim AS, Sulaiman WA, Zilfalil BA. Maternal uniparental heterodisomy of chromosome 6 in a boy with an isolated cleft lip and palate. Am J Med Genet A 2010: 152A (7): 1818–1821.
19. Turner CL, Mackay DM, Callaway JL et al. Methylation analysis of 79 patients with growth restriction reveals novelpatterns of methylation change at imprinted loci. Eur J Hum Genet 2010: 18: 648–655.
20. Maksimova N, Hara K, Miyashia A et al. Clinical, molecular and histopathological features of short stature syndrome with novel *CUL7* mutation in Yakuts: new population isolate in Asia. J Med Genet 2007: 44: 772–778.

Oikawa et al. Radiation Oncology 2011, 6:168
http://www.ro-journal.com/content/6/1/168

RADIATION ONCOLOGY

RESEARCH Open Access

Significance of genomic instability in breast cancer in atomic bomb survivors: analysis of microarray-comparative genomic hybridization

Masahiro Oikawa[1,2], Koh-ichiro Yoshiura[1], Hisayoshi Kondo[3], Shiro Miura[4], Takeshi Nagayasu[2] and Masahiro Nakashima[5*]

Abstract

Background: It has been postulated that ionizing radiation induces breast cancers among atomic bomb (A-bomb) survivors. We have reported a higher incidence of *HER2* and *C-MYC* oncogene amplification in breast cancers from A-bomb survivors. The purpose of this study was to clarify the effect of A-bomb radiation exposure on genomic instability (GIN), which is an important hallmark of carcinogenesis, in archival formalin-fixed paraffin-embedded (FFPE) tissues of breast cancer by using microarray-comparative genomic hybridization (aCGH).

Methods: Tumor DNA was extracted from FFPE tissues of invasive ductal cancers from 15 survivors who were exposed at 1.5 km or less from the hypocenter and 13 calendar year-matched non-exposed patients followed by aCGH analysis using a high-density oligonucleotide microarray. The total length of copy number aberrations (CNA) was used as an indicator of GIN, and correlation with clinicopathological factors were statistically tested.

Results: The mean of the derivative log ratio spread (DLRSpread), which estimates the noise by calculating the spread of log ratio differences between consecutive probes for all chromosomes, was 0.54 (range, 0.26 to 1.05). The concordance of results between aCGH and fluorescence in situ hybridization (FISH) for *HER2* gene amplification was 88%. The incidence of *HER2* amplification and histological grade was significantly higher in the A-bomb survivors than control group (P = 0.04, respectively). The total length of CNA tended to be larger in the A-bomb survivors (P = 0.15). Correlation analysis of CNA and clinicopathological factors revealed that DLRSpread was negatively correlated with that significantly (P = 0.034, r = -0.40). Multivariate analysis with covariance revealed that the exposure to A-bomb was a significant (P = 0.005) independent factor which was associated with larger total length of CNA of breast cancers.

Conclusions: Thus, archival FFPE tissues from A-bomb survivors are useful for genome-wide aCGH analysis. Our results suggested that A-bomb radiation may affect the increased amount of CNA as a hallmark of GIN and, subsequently, be associated with a higher histologic grade in breast cancer found in A-bomb survivors.

Keywords: breast cancer, atomic bomb survivors, radiation, genomic instability, CGH, microarray

Background

Genomic instability (GIN) is an important hallmark of an enhanced carcinogenic process in human. Although there are various forms of GIN, many cancer cells show higher rates of chromosomal instability, which means changes in chromosome structure and number, compared with normal cells [1]. Recent cytogenetic analysis revealed that there were equal numbers of cytogenetic aberrations in solid cancers and hematological malignancies [2]. Several previous studies have reported the association between chromosome instability and GIN/clinical phenotypes in breast cancers. Fridlyand et al. [3] categorized three breast tumor subtypes based on copy number aberrations (CNA) in tumor DNA, which includes DNA copy number gains and losses, and

* Correspondence: moemoe@nagasaki-u.ac.jp
[5]Department of Tumor and Diagnostic Pathology, Atomic Bomb Disease Institute, Nagasaki University Graduate School of Biomedical Sciences, Nagasaki, Japan
Full list of author information is available at the end of the article

suggested that these aberrations were related to shorter telomeres and the deregulation of the retinoblastoma (RB) gene pathway using an analysis of array comparative genomic hybridization (aCGH). Andre et al. [4] divided 106 breast cancers into three subtypes by the clustering method with the aCGH data and observed a correlation between cytogenetic subtypes and clinicopathologic characteristics, histological grade and intrinsic subtypes [5]. Hu et al. [6] and Melchor et al. [7] classified breast cancers by immunohistochemical staining pattern and found that triple-negative or basal-like subtype, which had the highest GIN among these subtypes, had the highest overall frequencies of CNA. Loo et al. [8] showed a correlation between fractional allelic loss and tumor size, mitotic rate and DNA content.

Atomic bomb (A-bomb) survivors who were exposed at young ages have already reached cancer-prone age. An increased risk of cancer has continued for decades, and the incidence of certain types of cancer is still higher in A-bomb survivors than in control populations [9-14]. It has been postulated that ionizing radiation induces breast cancers among A-bomb survivors. Our recent study demonstrated an association of *HER2* and *C-MYC* oncogene amplification in breast cancers among A-bomb survivors with radiation exposure [15]. Oncogene amplification is thought to be associated with GIN and a main characteristic of solid tumors [16]. It is conceivable that radiation from the A-bomb 65 years ago may have induced a higher level of GIN in A-bomb survivors as a long-lasting health effect which is associated with the development of oncogene amplifications and subsequent carcinogenesis. However, the crucial mechanisms that can account for a radiation effect inducing GIN on the whole genome of breast cancers in A-bomb survivors remains elusive.

The rapid progress of technological innovation in biomedical science has enabled CGH analysis to be performed with higher resolution using high density oligonucleotide microarrays [17]. However, utilizing formalin-fixed paraffin-embedded (FFPE) archival tissue for the aCGH, which is the most common form of tissue preservation in routine practice, remains challenging. The main obstacle is DNA degradation, such as cross-linking between nucleic acid strands, DNA adducts with histones or nucleic acid binding proteins, and breaking and depurination of DNA. Recently, a one-step chemical labeling method, called the Universal Linkage System (ULS), has been put into production. This method yields precise, robust and high-quality aCGH data by labeling DNA with fluorescent dyes at the N7 position of guanine without enzymatic reaction, which is subject to perturbation by degraded DNA [18-20].

In the present study, we analyzed FFPE archival breast cancer tissues from A-bomb survivors by aCGH using a high density oligonucleotide microarray and ULS labeling to determine the effect of A-bomb radiation on genomic alterations during breast carcinogenesis. This study revealed a higher incidence of CNA in breast cancer tissue from A-bomb survivors than in tissue from calendar year-matched control patients, suggesting a role for GIN during breast carcinogenesis in A-bomb survivors. To the best of our knowledge, this is the first report of an aCGH analysis with solid tumors from A-bomb survivors.

Methods

Tumor samples and clinical information

All samples were FFPE tissues. An A-bomb survivor was defined in the present study as a person who received the "Atomic Bomb Survivor's Health Handbook" produced by Nagasaki city authorities since the establishment of the Atomic Bomb Survivors' Medical Treatment Law in April 1957. Our previous report has already identified 35 breast cancers from A-bomb survivors exposed at or less than 1.5 km from the hypocenter in pathological records collected from 1961 to 1999 at the Nagasaki University Hospital [15]. The estimated doses in Nagasaki survivors who were not shielded at the time of explosion were 924.7 centigrays (cGy) at 1 km and 120.7 cGy at 1.5 km from the hypocenter [21]. Simultaneously, we have already analyzed *HER2* and *C-MYC* gene amplification by FISH method with FFPE samples and revealed that 26 out of 35 cases show clear hybridization signals for *HER2* and/or *C-MYC* gene amplification. In this study, 15 (mean age: 58.0 years, range: 45.4-82.8 years) out of 26 cases are available for aCGH analysis because there is a limit to the amount of tissues. As control subjects, 13 cases of invasive ductal carcinoma from calendar year-matched patients (matched on date of both diagnosis and birth; mean age: 55.5 years, range: 43.0-69.1 years), who did not receive "Health Handbook" according to the Atomic Bomb Survivors' Medical Treatment Law, were also analyzed. All clinicopathologic information including exposure distance, diagnosis, the modified Bloom-Richardson histologic grading, had been determined in our previous study [15]. Clinicopathological findings of these samples are provided in Additional file 1, Table S1. All experimental procedures for this study were approved by Committee for the Ethical Issues on Human Genome and Gene Analysis at Nagasaki University (Protocol No. 0305150036-2).

DNA extraction

Tumor DNA was extracted from FFPE archival tissues, as reported previously [22]. Briefly, using ten 10 μm-thick sections, tumor areas containing more than 70% tumor cells, identified by a guide slide stained with

hematoxylin and eosin, were microdissected from each FFPE block. Paraffin removal was performed in 80% xylene and tissues were washed twice with absolute ethanol, and deparaffinized tissue pieces were spun down. After drying, pellets were resuspended in 360 μL of buffer ATL (QIAmp DNA Mini Kit, Quiagen, Germany) and incubated at 95°C for 15 minutes, followed by cooling to room temperature. Samples were immediately digested with proteinase K for three days at 56°C in a rotation oven with periodic mixing and addition of fresh proteinase K every 24 hours. DNA was collected using the QIAmp DNA Mini Kit according to the manufacturer's instructions. Specifically, 400 μL of buffer AL (equal volume to sample suspension) was added to the sample and incubated at 70°C for 10 minutes. 400 μL of absolute ethanol was then added. The sample solution was then placed into the spin column and centrifuged for 1 minute at 8000 × g. The spin column was washed twice with 500 μL of buffer AW1 by centrifugation at 8000 × g for one minute and then washed with buffer AW2 by centrifugation at 14,000 × g for three minutes. The DNA was finally eluted with 55 μL buffer AE. Extracted DNA was quantified on a NanoDrop ND-1000 spectrophotometer (NanoDrop Technologies, Wilmington, DE, USA).

aCGH analysis

The Genomic DNA ULS Labeling Kit (Agilent technologies, USA) was used to chemically label 500 ng of tumor DNA from samples and from reference female genomic DNA (Promega, USA) with Cy5 or Cy3 dye for 30 minutes at 85°C, respectively, followed by purification using Agilent-KREA*pure*™ columns. Because ULS method labeled DNA with fluorescent dyes directly without any amplification steps or enzymatic reaction, this method is suitable for aCGH analysis using degraded DNA such as from FFPE blocks [18-20]. Dye-flip analyses were conducted on 6 of 28 samples, where samples were labeled with Cy3 and references were labeled with Cy5. Purified, labeled samples were then combined and mixed with human Cot-1 DNA (Invitrogen, USA), Agilent 10× Blocking Agent and Agilent 2× Hybridization Solution. Prior to array hybridization, hybridization mixtures were denatured at 95°C for 3 minutes and incubated at 37°C for 30 minutes. Agilent CGH*block* was added and samples were hybridized to the SurePrint G3 Human CGH 8 × 60 K Microarray, which contains 8 identical arrays consisting of ~63,000 in situ synthesized 60-mer oligonucleotide probes that span coding and noncoding sequences with an average spatial resolution of ~54 kb. Hybridization was carried out at 65°C for 40 hours before washing in Agilent Oligo aCGH Wash Buffer 1 at room temperature for 5 minutes, followed by washing in Agilent Oligo aCGH Wash Buffer 2 at 37°C for 1 minute.

Scanning and image analysis were done on an Agilent DNA Microarray Scanner. Feature Extraction Software (version 9.5) was used for data extraction from raw microarray image files. Agilent Genomic Workbench (version 5.0) was used to visualize, detect and analyze chromosomal patterns using an ADM-2 algorithm with the threshold set to 5.5. A copy number gain was defined as a log 2 ratio > 0.25 and a copy number loss was defined as a log 2 ratio < -0.25.

Statistical analysis

The total length of the CNA, which is the sum of each segment gained or lost, was used as an indicator of GIN. To determine the effect of each clinicopathological factor on the natural logarithm of GIN, Student's (Welch's) t-test or analysis of variance and the significance test of Pearson's correlation coefficient were performed. Means and proportions of each clinicopathological factor were compared between A-bomb survivors and control using t-tests, Fishers exact tests and Cochran-Armitage tests. We evaluated the impact of A-bomb exposure, age at the time of diagnosis, storage time, histological grade according to the modified Bloom-Richardson histologic grading system [23], derivative log ratio spread (DLRSpread), which estimates the log ratio noise by calculating the spread of log ratio differences between consecutive probes along all chromosomes, *HER2* amplification and *C-MYC* amplification determined by FISH on GIN using analysis of covariance which is a technique that combines the features of analysis of variance and regression. Our model was

$$Y_{ij} = \mu_i + \sum_{k=1}^{6} \beta_k (X_{kij} - \bar{X}_{k..}) + \varepsilon_{ij}$$

where Y_{ij} is the natural logarithm of GIN of the jth observation in the ith class and μ_i represents the population means of the A-bomb exposure classes, β_k is the regression coefficient of Y on X_k, ε_{ij} is the residual. Here, X_k is the variable which represents age at the time of diagnosis, DLRSpread, *HER2* amplification, *C-MYC* amplification, histological grade and storage time.

Effects were considered statistically significant when P-values were less than 0.05. The CORR, TTEST, FREQ and GLM procedures in the SAS system (version 9.1.3) was utilized for calculation.

Results

Results of aCGH analysis

The mean of the DLRSpread was 0.54 (range, 0.26 to 1.05) (Additional file 1, Table S1). As a quality assessment measure, we examined the concordance of the dye-flip analysis and the correlation between aCGH and

FISH results concerning *HER2* and *C-MYC* oncogene amplification. In the 6 samples with dye-flip analyses, the mean of the concordance rate of each paired sample was 76.0% (range, 43.2% to 96.1%) (Additional file 2, Table S2). The concordance rate of each paired sample was defined as the ratio of length of copy number aberrant region in one dye combination to the dye-flipped combination in each sample. To confirm the validity of aCGH results using FFPE samples, we compared the results of amplification status of *HER2* and *C-MYC* in the aCGH and FISH results. *HER2* was amplified in 9 of 25 samples, in which showed clear hybridization signals in the FISH analysis. In 7 of these 9 samples, the log 2 ratio for the probe sets (A_14_P121276, A_14_P114826 and triplicate of A_16_P20643178) corresponding to the *HER-2* gene was > 0.25, which met our criteria for a gain based on aCGH results. The sensitivity, specificity and overall accuracy for the *HER2* gene were 77.8%, 93.8% and 88%, respectively (Additional file 3, Figure S1). Whereas *C-MYC* was amplified in 11 of 23 samples, in which showed clear hybridization signals in the FISH analysis, only two of these 11 samples showed a gain for the probe sets (A_14_P128991, A_14_P138867 and A_14_P137636) corresponding to the *C-MYC* gene based on aCGH results. The sensitivity, specificity and overall accuracy for the *C-MYC* gene were 18%, 75% and 48%, respectively (Additional file 4, Figure S2).

In our detection setting, the ADM-2 algorithm with the threshold set to 5.5, CNA were detected in all samples. The mean of the total number of site and the length of CNA were 10.29 (range, 1 to 28) and 105,400,874 bp (range, 607,921 bp to 525,839,497), respectively (Additional file 1, Table S1), and these values varied from case to case (Additional file 5, Figure S3).

Correlation between GIN and clinicopathological findings

The results of comparisons of clinicopathological profiles of breast cancer between A-bomb survivors and control are shown in Table 1. Proportions of histological grade and the incidence of HER2 amplification were significantly higher in A-bomb survivors than in controls (P = 0.04, P = 0.04, respectively), which is consistent with our data published previously [15]. The total length and number of CNA tended to be larger in the A-bomb survivors (P = 0.15, P = 0.16, respectively).

The correlations between the total length of CNA and histological subtypes, histological grade, status of axillary lymph node metastasis, status of estrogen receptor (ER), *HER2/C-MYC* amplifications determined by FISH, age at the time of diagnosis, tumor size, age of samples, DLRSpread, age of the time at the A-bomb exposure, the exposure distance from the hypocenter and time between age at diagnosis and age at exposure were tested (Table 2, Table 3). Among these factors, DLRSpread was negatively correlated with the total length of CNA significantly (P = 0.034, r = -0.40) and age at the time of diagnosis, age of samples tended to be correlated with that negatively (P = 0.055, r = -0.37) and positively (P = 0.064, r = 0.35), respectively. Notably, among A-bomb survivors, latent period from irradiation was inversely correlated with the total length of CNA, indicating an involvement of GIN in the case of breast cancer which showed early onset from an initiation event by A-bomb exposure.

The multivariate analysis using analysis of covariance revealed that the status of A-bomb exposure was the most significant factor for the total length of CNA even excluding the effect of *HER2* and *C-MYC* amplification, histological grade, age at the time of diagnosis, age of samples and DLRSpread (Figure 1, Table 4). Analysis of covariance-adjusted difference in means between the A-bomb exposed group and the unexposed group is 63,151,697 (95%CI, 18,291,298 to 151,682,068; P = 0.005) for GIN.

Discussion

Ionizing radiation is an established risk factor for breast cancers [24-27]. Several epidemiologic reports have suggested that an increased risk of cancer has continued for decades after exposure, and that a higher risk of certain types of cancers still persists in A-bomb survivors [9-14]. Thus, a long-lasting health effect is considered to be a contributing factor in tumorigenesis in A-bomb survivors. We have recently demonstrated an association of oncogene amplification in breast cancers among A-bomb survivors with radiation exposure [15], which can be regarded as being the results of positive selection during breast carcinogenesis. This finding suggests that A-bomb radiation may affect the development of oncogene amplification by inducing a higher level of GIN in breast cancers found in survivors. The current study was carried out to further confirm the enhanced GIN in A-bomb radiation-associated breast cancers using the aCGH method. The aCGH method is a quite useful technique to detect the DNA CNA as an indicator of GIN, which represents chromosomal loss and gain caused by radiation-induced DNA double-strand breaks [16]. Unger et al. [28] found DNA CNA pattern which is characteristic of radiation-induced papillary thyroid cancer in residents living in the vicinity of Chernobyl using the aCGH method.

Tissue samples from A-bomb survivors are considered to be extremely valuable biological materials with which to analyze the radiation signature or radiation-associated human health effects, particularly in low-dose and late exposures. The molecular analyses of carcinogenesis in A-bomb survivors require clinical data of individuals and biological materials with pathologic data of tumors.

Table 1 Comparisons of clinicopathological factors of breast cancers between A-bomb survivor and control.

Clinicopathological profile	A-bomb survivors (n = 15)	Control (n = 13)	*P*-value
Mean age of onset (years old)	58.0 (52.6, 63.4)†	55.5 (49.7, 61.4)	0.51[1)]
Mean tumor size (cm)	24.7 (20.7, 28.8)	36.2 (20.2, 52.3)	0.15[1)]
Histological subtype			
Papillo-tubular	9	4	0.29[2)]
Solid-tubular	1	2	
Scirrhous	5	7	
Histological grade			
I	1	3	0.04[3)]
II	5	7	
III	9	3	
Lymph node metastasis			
Positive	8	5	0.60[4)]
Negative	4	4	
Unknown	3	4	
ER status			
Positive	7	8	0.26[4)]
Negative	8	5	
PgR status			
Positive	7	8	0.43[4)]
Negative	8	5	
HER2 amplification (FISH)			
Positive	7	2	0.04[4)]
Negative	5	11	
No signal	3	0	
C-MYC amplification (FISH)			
Positive	9	2	0.09[4)]
Negative	5	7	
No signal	1	4	
Mean total length of CNA (bp)	64,032,415 (29,443,979, 139,238,660)	23,924,175 (6,936,445, 82,515,771)	0.15[1)]
Mean number of CNA	12.2 (8.4, 16.0)	8.08 (3.0, 13.1)	0.16[1)]

†: 95% confidence interval, CNA: copy number aberrations

1): t-test, 2): χ^2-test, 3): Cochran-Armitage test, 4): Fisher's exact test

Our database, which consist of two independent databases: a clinical database providing exposure distance on Nagasaki survivors registered at our institute which was established in 1972 and a pathological database by the Nagasaki Tumor Tissue Registry (NTTR) which was established in 1974, allow us to obtain FFPE archival tissue samples resected from A-bomb survivors. For the genomic analyses, we confirmed the utility of FFPE archival tissue with FISH methods to detect gene amplification despite DNA degradation caused by fixation and long storage. In the present study, we conducted an aCGH analysis using tumor DNA extracted from FFPE archival breast cancer samples from A-bomb survivors. To our knowledge, this is the first attempt to perform an aCGH analysis with solid tumors from A-bomb survivors. The samples used in this study were very old, with ranges 14 to 43 years (with a mean of 25 years) in storage. The DLRSpread obtained was 0.26 to 1.05, with a mean of 0.54, which indicated the relatively lower quality of this experiment compared with that expected with DNA from fresh frozen tissue or peripheral blood lymphocyte. However, the status of *HER2* oncogene amplification based on aCGH result was highly concordant with the results of FISH that the sensitivity, specificity and accuracy were 77.8%, 93.8% and 88%, respectively, which were comparable to the results from former aCGH studies with FFPE archival tissue [29,30]. By contrast, the concordance was low for the status of *C-MYC* oncogene amplification between the results from aCGH and FISH, with the sensitivity, specificity and accuracy being 18%, 75% and 48%, respectively. This discordance, especially in sensitivity, may result from the use of only three probes on the *C-MYC* gene and a smaller change in amplification at the region including *C-MYC* than the *HER2* gene. Our results suggest that the 60K×8 CGH array is a reliable technology

Table 2 Comparisons of total length of copy number aberrations (CNA) by clinicopathological factor of breast cancers.

Clinicopathological factor	Total (N = 28) n (%)	Mean total length of CNA (bp)	*P*-value
Histological subtype			
Papillo-tubular	13 (46)	27,487,678	0.54[1)]
Solid-tubular	3 (11)	41,158,092	
Scirrhous	12 (43)	61,520,542	
Histological grade			
I	4 (14)	49,011,523	0.32[2)]
II	12 (43)	47,158,730	
III	12 (43)	32,711,871	
Axillary lymph node metastasis			
Positive	13 (62)	30,993,870	0.30[3)]
Negative	8 (38)	59,602,019	
ER status			
Positive	14 (50)	53,249,555	0.43[3)]
Negative	14 (50)	30,863,969	
HER2 amplification (FISH)			
Positive	9 (36)	28,970,829	0.75[3)]
Negative	16 (64)	37,017,451	
C-MYC amplification (FISH)			
Positive	11 (48)	38,698,059	0.46[3)]
Negative	12 (52)	22,102,472	

1): analysis of variance, 2): Jonckheere-Terpstra trend test, 3): t-test

to identify gene copy number aberration with definite changes.

Our aCGH analysis showed a great deal of variety in its amount and pattern of genomic alterations from case to case. In comparison with previous reports on breast cancers from general population, mean number of CNA in our cases seemed to be relatively small (mean: 12.2, range: 2-28) but recurrently affected regions (8q24.3, 17q12, 19p13.11, 1q21.2-q22: Additional file 5, Figure S3) found in our cases were concordant [4,7,31-33]. However, direct comparisons of the current results with published results in aCGH are practically difficult because the results of aCGH analyses are greatly influenced by the array design and type of samples (e.g., fresh frozen or FFPE). A previous study of an aCGH analysis of radiation-induced and spontaneous rat mammary carcinoma indicated that the frequency of carcinoma having any CNA and the number of CNA in radiation-induced carcinoma were significantly greater than that observed in the spontaneous carcinoma [34]. Another study of an aCGH analysis of premenopausal breast cancers in the residents from a nuclear fallout-contaminated area in Belarus did not show any significant differences or tendencies in the average number of

Table 3 Correlation analyses between clinicopathological factors and total length of copy number aberrations in breast cancers.

Clinical factors	Mean total length of copy number aberrations (bp)			
	All cases (n = 28)		A-bomb survivors (n = 15)	
	r*	*P*-value*	r*	*P*-value*
Age at the time of diagnosis	-0.37	0.055	-0.59	0.021
Tumor size (cm)	0.042	0.83	-0.25	0.37
Storage time (years)	0.35	0.064	0.49	0.067
DLRSpread	-0.40	0.034	-0.38	0.16
Age of the time of exposure to the A-bomb**			-0.31	0.25
Exposure distance from the hypocenter (km)**			0.11	0.70
Time between age at diagnosis and exposure (year)**			-0.52	0.047

*Pearson's correlation coefficient. **Only among A-bomb survivors

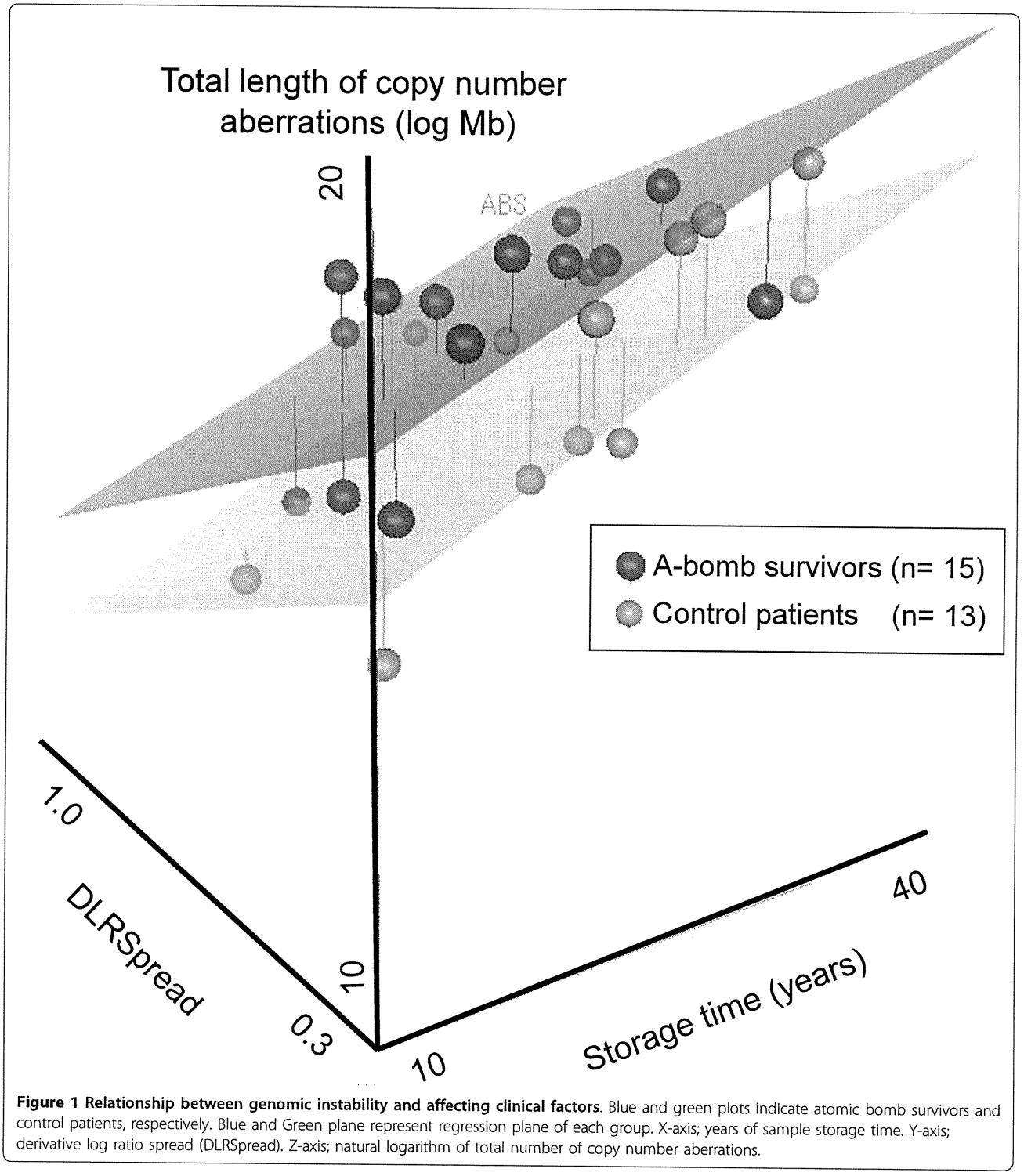

Figure 1 Relationship between genomic instability and affecting clinical factors. Blue and green plots indicate atomic bomb survivors and control patients, respectively. Blue and Green plane represent regression plane of each group. X-axis; years of sample storage time. Y-axis; derivative log ratio spread (DLRSpread). Z-axis; natural logarithm of total number of copy number aberrations.

total DNA CNA compared with matched control cases from Western New York, even though breast cancer from Belarus had significantly more average number of gains [35]. These discrepancies may result from differences in the experimental models, since the former is a study of a simplified animal cancer model and the latter is an observational study of human cancer affected by many etiological factors. But the present study endorsed the former result with a tendency for breast cancer in A-bomb survivors to have a higher number of CNA (P = 0.16, Table 1, Additional file 1, Table S1). Furthermore, mean total length of CNA were also larger, if not

Table 4 Multivariate analyses with covariance in total length of copy number aberrations in breast cancers.

Source of Variation	DF*	Mean Squares	*F*-value	*P*-value*
A-bomb exposure	1	20.59	11.62	0.005
HER2 amplification (FISH)	1	0.65	0.37	0.556
C-MYC amplification (FISH)	1	4.14	2.34	0.152
Histological Grade	1	1.06	0.60	0.454
Age at the time of diagnosis	1	2.35	1.32	0.272
Storage time (years)	1	8.78	4.96	0.046
DLRSpread	1	3.77	2.13	0.170

*Degrees of Freedom

significantly, in the A-bomb survivors than control group (P = 0.15, Table 1, Additional file 1, Table S1). Herein, we assumed the total length of CNA as an indicator of GIN because the amount of CNA represents the consequences of double-strand breaks, abnormal DNA damage repairs and gross rearrangements of chromosomes [1,16], and a consecutive changes of probes is considered to be much more important than a change of only one probe in such experimental model using high density probes and relatively noisy data. Since high histological grade, ER negative expression, early age of onset and *HER2* amplification were reported to be correlated with higher incidence of genomic aberrations [4], we examined the correlation between the total length of CNA and clinicopathological factors, followed by multivariate analysis using analysis of covariance to evaluate the impact (effect) of A-bomb exposure, age at the time of diagnosis, HER2 and C-MYC amplification, histological grade, storage time, and DLRSpread on GIN, which have shown that the status of A-bomb exposure showed a significant correlation after the exclusion of confounding factor by the multivariate analysis (Table 4). Thus, we have demonstrated that breast cancers in A-bomb survivors harbored significant GIN independently of the effect of other clinicopathological factors.

Conclusions

The present study indicated that archival FFPE tissues from A-bomb survivors are useful for genome-wide aCGH analysis and A-bomb radiation exposure induced GIN not only at the region of the *HER2* and *C-MYC* oncogenes but throughout the whole genome in breast cancers by aCGH. The crucial mechanisms that can account for the continuously higher incidence of breast cancers in A-bomb survivors for decades remain to be determined. Further research on the molecular mechanisms to induce a long-lasting GIN in the breast tissue from survivors can contribute to an understanding of radiation-associated carcinogenesis.

Additional material

Additional file 1: Table S1. Summary of clinicopathological factors and aCGH Analysis.

Additional file 2: Table S2. Result of dye-flip analysis.

Additional file 3: Figure S1. Chromosomal view of chromosome 17 and comparison of the results from FISH and aCGH analyses on *HER2* oncogene. Log2 ratio values for all oligonucleotide probes are plotted as a function of their chromosomal position. Each point represents a single probe and the blue vertical line indicates the position of the *HER2* oncogene. Aberration calls identified by ADM-2 algorithm are shown.

Additional file 4: Figure S2. Chromosomal view of chromosome 8 and comparison of the results from FISH and aCGH analyses on *C-MYC* ongcogene. Log2 ratio values for all oligonucleotide probes are plotted as a function of their chromosomal position. Each point represents a single probe and the blue vertical line indicates the position of the *C-MYC* oncogene. Aberration calls identified by ADM-2 algorithm are shown.

Additional file 5: Figure S3. Graphic display of whole genomic aberrations in atomic bomb survivors (upper panel) and control patients (lower panel). The panels to the right of each chromosome shows the frequency of gains, indicated by the red bars ranging from 0% to 100%, and losses, indicated by the green bars ranging from 0% to 100%.

Acknowledgements

This work was supported in part through Nagasaki University Global Center of Excellence (COE) program, by Grant-in-Aid for Scientific Research from the Japanese Ministry of Education, Science, Sports and Culture (No. 19790263), and by Grant for Research Project of Atomic Bomb Diseases from the Japanese Ministry of Health, Labour and Welfare.

We are grateful to the patients for their participation in this research. We also thank Ms Chisa Hayashida and Ms Maiko Kawamichi for their technical assistance.

Author details

[1]Department of Human Genetics, Atomic Bomb Disease Institute, Nagasaki University Graduate School of Biomedical Sciences, Nagasaki, Japan. [2]Department of Surgical Oncology, Nagasaki University Graduate School of Biomedical Sciences, Nagasaki, Japan. [3]Biostatistics Section, Division of Scientific Data Registry, Atomic Bomb Disease Institute, Nagasaki University Graduate School of Biomedical Sciences, Nagasaki, Japan. [4]Tissue and Histopathology Section, Division of Scientific Data Registry, Atomic Bomb Disease Institute, Nagasaki University Graduate School of Biomedical Sciences, Nagasaki, Japan. [5]Department of Tumor and Diagnostic Pathology, Atomic Bomb Disease Institute, Nagasaki University Graduate School of Biomedical Sciences, Nagasaki, Japan.

Authors' contributions

MO participated in the design of the study and carried out aCGH analysis. KY participated in the design of the study. HK performed the statistical analysis. SM conducted pathological analysis. TN participated in the design of the study. MN conceived of the study and participated in the design of the study. All authors read and approved the final manuscript.

Competing interests

The authors declare that they have no competing interests.

Received: 14 September 2011 Accepted: 7 December 2011
Published: 7 December 2011

References

1. Negrini S, Gorgoulis VG, Halazonetis TD: **Genomic instability–an evolving hallmark of cancer.** *Nat Rev Mol Cell Biol* 2010, 11(3):220-228.

2. Mitelman F, Johansson B, Mertens F: **Fusion genes and rearranged genes as a linear function of chromosome aberrations in cancer.** *Nat Genet* 2004, **36(4)**:331-334.
3. Fridlyand J, Snijders AM, Ylstra B, Li H, Olshen A, Segraves R, *et al*: **Breast tumor copy number aberration phenotypes and genomic instability.** *BMC Cancer* 2006, **6**:96.
4. Andre F, Job B, Dessen P, Tordai A, Michiels S, Liedtke C, *et al*: **Molecular characterization of breast cancer with high-resolution oligonucleotide comparative genomic hybridization array.** *Clin Cancer Res* 2009, **15(2)**:441-451.
5. Sorlie T, Tibshirani R, Parker J, Hastie T, Marron JS, Nobel A, *et al*: **Repeated observation of breast tumor subtypes in independent gene expression data sets.** *Proc Natl Acad Sci USA* 2003, **100(14)**:8418-8423.
6. Hu X, Stern HM, Ge L, O'Brien C, Haydu L, Honchell CD, *et al*: **Genetic alterations and oncogenic pathways associated with breast cancer subtypes.** *Mol Cancer Res* 2009, **7(4)**:511-522.
7. Melchor L, Honrado E, Garcia MJ, Alvarez S, Palacios J, Osorio A, *et al*: **Distinct genomic aberration patterns are found in familial breast cancer associated with different immunohistochemical subtypes.** *Oncogene* 2008, **27(22)**:3165-3175.
8. Loo LW, Ton C, Wang YW, Grove DI, Bouzek H, Vartanian N, *et al*: **Differential patterns of allelic loss in estrogen receptor-positive infiltrating lobular and ductal breast cancer.** *Genes Chromosomes Cancer* 2008, **47(12)**:1049-1066.
9. Preston DL, Shimizu Y, Pierce DA, Suyama A, Mabuchi K: **Studies of mortality of atomic bomb survivors. Report 13: Solid cancer and noncancer disease mortality: 1950-1997.** *Radiat Res* 2003, **160(4)**:381-407.
10. Ron E, Lubin JH, Shore RE, Mabuchi K, Modan B, Pottern LM, *et al*: **Thyroid cancer after exposure to external radiation: a pooled analysis of seven studies.** *Radiat Res* 1995, **141(3)**:259-277.
11. Nakashima M, Kondo H, Miura S, Soda M, Hayashi T, Matsuo T, *et al*: **Incidence of multiple primary cancers in Nagasaki atomic bomb survivors: association with radiation exposure.** *Cancer Sci* 2008, **99(1)**:87-92.
12. Carmichael A, Sami AS, Dixon JM: **Breast cancer risk among the survivors of atomic bomb and patients exposed to therapeutic ionising radiation.** *Eur J Surg Oncol* 2003, **29(5)**:475-479.
13. Preston DL, Ron E, Tokuoka S, Funamoto S, Nishi N, Soda M, *et al*: **Solid cancer incidence in atomic bomb survivors: 1958-1998.** *Radiat Res* 2007, **168(1)**:1-64.
14. Land CE, Tokunaga M, Koyama K, Soda M, Preston DL, Nishimori I, *et al*: **Incidence of female breast cancer among atomic bomb survivors, Hiroshima and Nagasaki, 1950-1990.** *Radiat Res* 2003, **160(6)**:707-717.
15. Miura S, Nakashima M, Ito M, Kondo H, Meirmanov S, Hayashi T, *et al*: **Significance of HER2 and C-MYC oncogene amplifications in breast cancer in atomic bomb survivors: associations with radiation exposure and histologic grade.** *Cancer* 2008, **112(10)**:2143-2151.
16. Mondello C, Smirnova A, Giulotto E: **Gene amplification, radiation sensitivity and DNA double-strand breaks.** *Mutat Res* 2008, **704(1-3)**:29-37.
17. Barrett MT, Scheffer A, Ben-Dor A, Sampas N, Lipson D, Kincaid R, *et al*: **Comparative genomic hybridization using oligonucleotide microarrays and total genomic DNA.** *Proc Natl Acad Sci USA* 2004, **101(51)**:17765-17770.
18. Raap AK, van der Burg MJ, Knijnenburg J, Meershoek E, Rosenberg C, Gray JW, *et al*: **Array comparative genomic hybridization with cyanin cis-platinum-labeled DNAs.** *Biotechniques* 2004, **37(1)**:130-134.
19. Joosse SA, van Beers EH, Nederlof PM: **Automated array-CGH optimized for archival formalin-fixed, paraffin-embedded tumor material.** *BMC Cancer* 2007, **7**:43.
20. Knijnenburg J, van der Burg M, Tanke HJ, Szuhai K: **Optimized amplification and fluorescent labeling of small cell samples for genomic array-CGH.** *Cytometry A* 2007, **71(8)**:585-591.
21. Sadamori N, Shibata S, Mine M, Miyazaki H, Miyake H, Kurihara M, *et al*: **Incidence of intracranial meningiomas in Nagasaki atomic-bomb survivors.** *Int J Cancer* 1996, **67(3)**:318-322.
22. Oikawa M, Ngayasu T, Yano H, Hayashi T, Abe K, Kinoshita A, *et al*: **papillary carcinoma of breast hharbors significant genomic alteration compared with intracystic papilloma: Genome-wide copy number and LOH analysis using high-density single-nucleotide polymorphism microarrays.** *Breast J* 2011, **17(4)**:427-430.
23. Robbins P, Pinder S, de Klerk N, Dawkins H, Harvey J, Sterrett G, *et al*: **Histological grading of breast carcinomas: a study of interobserver agreement.** *Hum Pathol* 1995, **26(8)**:873-879.
24. Henderson TO, Amsterdam A, Bhatia S, Hudson MM, Meadows AT, Neglia JP, *et al*: **Systematic review: surveillance for breast cancer in women treated with chest radiation for childhood, adolescent, or young adult cancer.** *Ann Intern Med* 2010, **152(7)**:444-455, W144-454.
25. Clemons M, Loijens L, Goss P: **Breast cancer risk following irradiation for Hodgkin's disease.** *Cancer Treat Rev* 2000, **26(4)**:291-302.
26. Travis LB, Hill DA, Dores GM, Gospodarowicz M, van Leeuwen FE, Holowaty E, *et al*: **Breast cancer following radiotherapy and chemotherapy among young women with Hodgkin disease.** *Jama* 2003, **290(4)**:465-475.
27. Clarke M, Collins R, Darby S, Davies C, Elphinstone P, Evans E, *et al*: **Effects of radiotherapy and of differences in the extent of surgery for early breast cancer on local recurrence and 15-year survival: an overview of the randomised trials.** *Lancet* 2005, **366(9503)**:2087-2106.
28. Unger K, Malisch E, Thomas G, Braselmann H, Walch A, Jackl G, *et al*: **Array CGH demonstrates characteristic aberration signatures in human papillary thyroid carcinomas governed by RET/PTC.** *Oncogene* 2008, **27(33)**:4592-4602.
29. Paris PL, Sridharan S, Scheffer A, Tsalenko A, Bruhn L, Collins C: **High resolution oligonucleotide CGH using DNA from archived prostate tissue.** *Prostate* 2007, **67(13)**:1447-1455.
30. Jacobs S, Thompson ER, Nannya Y, Yamamoto G, Pillai R, Ogawa S, *et al*: **Genome-wide, high-resolution detection of copy number, loss of heterozygosity, and genotypes from formalin-fixed, paraffin-embedded tumor tissue using microarrays.** *Cancer Res* 2007, **67(6)**:2544-2551.
31. Cingoz S, Altungoz O, Canda T, Saydam S, Aksakoglu G, Sakizli M: **DNA copy number changes detected by comparative genomic hybridization and their association with clinicopathologic parameters in breast tumors.** *Cancer Genet Cytogenet* 2003, **145(2)**:108-114.
32. Naylor TL, Greshock J, Wang Y, Colligon T, Yu QC, Clemmer V, *et al*: **High resolution genomic analysis of sporadic breast cancer using array-based comparative genomic hybridization.** *Breast Cancer Res* 2005, **7(6)**: R1186-1198.
33. Nessling M, Richter K, Schwaenen C, Roerig P, Wrobel G, Wessendorf S, *et al*: **Candidate genes in breast cancer revealed by microarray-based comparative genomic hybridization of archived tissue.** *Cancer Res* 2005, **65(2)**:439-447.
34. Iizuka D, Imaoka T, Takabatake T, Nishimura M, Kakinuma S, Nishimura Y, *et al*: **DNA copy number aberrations and disruption of the p16Ink4a/Rb pathway in radiation-induced and spontaneous rat mammary carcinomas.** *Radiat Res* 2010, **174(2)**:206-215.
35. Varma G, Varma R, Huang H, Pryshchepava A, Groth J, Fleming D, *et al*: **Array comparative genomic hybridisation (aCGH) analysis of premenopausal breast cancers from a nuclear fallout area and matched cases from Western New York.** *Br J Cancer* 2005, **93(6)**:699-708.

doi:10.1186/1748-717X-6-168
Cite this article as: Oikawa *et al.*: Significance of genomic instability in breast cancer in atomic bomb survivors: analysis of microarray-comparative genomic hybridization. *Radiation Oncology* 2011 **6**:168.

Exp Oncol 2011
33, 1, 42–46

Experimental ONCOLOGY

DOWN-REGULATION OF ABCC11 PROTEIN (MRP8) IN HUMAN BREAST CANCER

*N. Sosonkina[1], M. Nakashima[2], T. Ohta[1], N. Niikawa[1], D. Starenki[1]**

[1]*Research Institute of Personalized Health Science, Health Sciences University of Hokkaido, Tobetsu, Hokkaido 061-0293, Japan*

[2]*Departments of Molecular Pathology, Nagasaki University Graduate School of Biomedical Science, Nagasaki 852-8523, Japan*

Aim: **To investigate the expression of ABCC11 (MRP8) protein in normal breast tissue, and examine the difference in *ABCC11* mRNA and protein expression between normal breast and breast cancer tissues taking into account *ABCC11* genotype (a functional SNP, rs17822931) and estrogen receptor (ER) status.** ***Methods***: **Sections of paraffin-embedded normal and malignant tissues from 10 patients with invasive ductal carcinoma were used for immunohistochemical analysis. DNA and RNA were extracted from the same sections and used for genotyping and *ABCC11* transcript expression measurement by quantitative RT-PCR.** ***Results***: **A strong expression of ABCC11 was found in epithelial and myoepithelial cells of normal breast lobules and ducts in individuals with different *ABCC11* genotypes. A predominant decrease of ABCC11 expression was observed in malignant tissue compared to normal beast specimen (8 of 10 cases), despite four out of ten tumors showed the elevated *ABCC11* mRNA level as compared to the normal counterpart. Neither *ABCC11* mRNA nor protein expression in normal or cancerous tissue correlated with ER status.** ***Conclusion***: **The expression of ABCC11 protein appears to be decreased in most BC. The effect of ABCC11 protein on breast cancer chemosensitivity is likely to be more complex than that which can be directly inferred from *ABCC11* genotype and mRNA expression level in the tumor.**
***Key Words: ABCC11* mRNA expression, MRP8 expression, normal breast, breast cancer.**

Human ATP-binding cassette (ABC) transport proteins have an essential function of extruding toxins from cells [1]. Namely this function brings ABC transporters into the focus of the studies of multidrug resistance of tumor cells. Starting with the *ABCB1* gene product, MDR1, several other transporters have been shown to cause anti-cancer drug resistance in cell culture through an increased efflux and decreased intracellular accumulation of chemotherapeutic agent [2]. Most ABC transporters associated with tumor resistance belong to the ABCC subfamily.

The *ABCC11* gene product (also known as MRP8) is one of nine multidrug resistances (MDR)-associated proteins of the ABCC subfamily. ABCC11 substrates include cyclic nucleotides, monoanionic bile acids, steroid sulfates, estradiol 17-β-D-glucuronide [3–4]. ABCC11 has been proved to confer resistance to chemotherapeutic drugs 5-fluorouracil (5-FU) [5] and pemetrexed (MTA, Alimta) [6].

Profiling of MDR proteins expression in cancer cells is an important direction in exploring of drug resistance mechanisms and discovering biomarkers of a particular tumor type. Breast cancer (BC), as the most common type of non-skin cancer in women and the fifth most common cause of cancer death, involves an intense research effort in this regard. Apart from MDR1 [7], no evidence has been reported yet on the relationship of ABC transporters with drug resistance of BC cells. At the same time, MDR genes transcripts, including *ABCC11* mRNA, have been shown to be over-expressed in BC [8–9]. Elevated expression levels of *ABCC11* in estrogen receptor (ER)α-positive, as compared to ERα-negative BC, were reported by Honorat *et al.* [10]. The authors also observed the regulation of the *ABCC11* expression by estrogen in MCF7 breast cancer cell line [10]. However, no studies addressing differential *ABCC11* expression in normal and cancerous breast tissues have been done so far. Similarly, nothing currently is known about the ABCC11 protein expression in normal breast tissue in comparison to the tumor.

This work was set out to examine the *ABCC11* transcript and ABCC11 protein expression in BC and matched normal breast specimens in 10 women in relation with ER status. We also analyzed *ABCC11* expression levels with regard to a functional SNP (rs17822931) in the *ABCC11* gene that apparently affects the transport activity of the protein [11–14].

MATERIALS AND METHODS

Samples. The study protocol was approved by the Committee for the Ethical Issues of Human Genome and Gene Analysis of Health Sciences University of Hokkaido. A total of 10 BC and normal mammary gland specimens which were located away from the tumor of the same patient were selected from pathological archives of the Department of Molecular Pathology, Atomic Bomb Disease Institute, Nagasaki University, Japan. Clinicopathological information on BC samples including ER status (positive/negative, as a part of routine pathological diagnosis of BC) was obtained from patients' records. Serial 5 μm sections of normal tissue and BC surgical specimen mounted on microscope slides were available for the study. Sections of all speci-

Received: February 14, 2011.
*Correspondence: Fax: 0133-23-1782;
E-mail: starenki@hoku-iryo-u.ac.jp

Abbreviations used: BC – breast cancer; ER – estrogen receptor; FFPE – formalin-fixed paraffin-embedded; MPR – multidrug resistance protein; SNP – single nucleotide polymorphism.

mens were stained with hematoxylin and eosin and re-analyzed by an experienced pathologist to confirm that each BC specimen contained cancerous tissue, and each normal breast sample was free of malignant tissue.

DNA extraction and genotyping. DNA was extracted from paraffin-embedded sections with DEXPAT reagent (TaKaRa Bio Inc., Otsu, Japan) according to the manufacturer's protocol. DNA was further precipitated with ethanol, reconstituted in TE buffer and 2 µl was used as a template in genotyping reactions. The samples were genotyped by TaqMan™ assay using the reagents, primers and probes (Applied Biosystems by Life Technologies, Foster City, CA, USA) and thermal cycling conditions described in our recent work [15]. The assays were run in a Rotor-Gene Q (QIAGEN, Tokyo, Japan). Four replicates of each sample were analyzed. Genotypes were assessed by automated allelic discrimination analysis and by comparison with external controls with known genotypes.

Quantitative real-time (qRT)-PCR. RNA was extracted from FFPE sections mounted on microscope slides with RNeasy FFPE kit (QIAGEN, Tokyo, Japan) according to the manufacturer's protocol with additional 3 min incubations at 50 ºC after adding of 1 ml of xylene, and before the first centrifugation step. cDNA was then synthesized using SuperScript First-Strand Synthesis System for RT-PCR (Invitrogen, Carlsbad, CA, USA). Three independent reverse-transcription reactions were done for each sample, and the content of each of the three tubes was used as an individual template in triplicate qRT-PCR. Commercially available TaqMan® Gene Expression Assays (Applied Biosystems by Life Technologies, Foster City, CA, USA) were used to analyze the target (*ABCC11* and *ESR1*) and reference cDNAs (*MRLP19*, *TBP*, *TFRC*). The respective assay IDs are listed in Table.

Table. Gene Expression Assays used as primers for quantitative RT-PCR

Gene symbol	Assay ID
ABCC11	Hs01090769_m1
ESR1	Hs00174860_m1
MRLP19	Hs00608522_m1
TBP	Hs00427621_m1
TFRC	Hs00951083_m1

Note: Assays were purchased from Applied Biosystems by Life Technologies (Foster City, CA, USA).

MRLP19, *TBP* and *TFRC* were selected as reference genes for normalization according to Drury *et al.* [16], who found these to be particularly suitable for gene expression analysis in FFPE material. To meet another important condition for qRT-PCR of FFPE samples [17], expression assays for all genes were selected to amplify the target as close to the 3' end as possible. To comply with the MIQE Guidelines [18], each set of primers was tested for efficacy using serial dilutions of a control cDNA sample. Reaction was performed in TaqMan® Universal PCR Master Mix (Applied Biosystems by Life Technologies, Foster City, CA, USA) under the following thermal profile: after the initial incubation at 50 ºC for 2 min followed by 95 ºC for 10 min, reaction was cycled 55 times at 95 ºC for 15 sec and at 60 ºC for 1 min in a Rotor-Gene Q machine. Geometrical mean of the relative concentrations of *ABCC11* and *ESR1* against each of *MRLP19*, *TBP*, and *TFRC* was used as the expression index in further analysis.

Antibodies. The ERα was detected in human breast tissues with a mouse monoclonal antibody NCL-ER-6F11 (Novocastra Laboratories, Newcastle, UK) diluted 1:80. ABCC11 was detected with rabbit polyclonal antibody provided by Dr. K.Yoshiura at the dilution of 1:100. For the immunofluorescent detection of the proteins, we used secondary anti-mouse –Alexa Fluor 594 and anti-rabbit –Alexa Fluor 488 (Invitrogen, Carlsbad, CA, USA) conjugates at 1:200 dilution. All antibodies were diluted in 1% BSA (Sigma, St Louis, MO, USA) in 0.01M PBS.

Immunohistochemical double labeling for ER and ABCC11. Sections of paraffin-embedded tissues were mounted on aminoalkylsilane-coated slides, deparaffinized, and rehydrated. The sections were sequentially incubated in four changes of boiling 0.01 M citrate buffer, pH 6.0, 5 min each, 2% hydrogen peroxide at room temperature for 15 min, three changes of PBS, 5 min each, and in 5% BSA blocking solution at room temperature for 20 min. Then the slides were washed in PBS for 10 min and incubated overnight at 4 °C in the mixture of primary anti-ER and anti-ABCC11 antibodies diluted as described above. After incubation the sections were washed in three changes of PBS, 10 min each, followed by 30 min incubation at room temperature with the mixture of the secondary antibodies. The slides were then rinsed in four changes of PBS, covered with Vectashield H-1200/DAPI mounting media (Vector Laboratories, Burlingame, CA, USA) and analyzed under a Biorevo BZ-9000 (Keyence Corp., Woodcliff Lake, NJ, USA) fluorescent microscope. The three-color images were acquired, merged and processed to remove haze and adjust the background using the built-in software. Green fluorescence intensity (ABCC11) was measured in the images and normalized to blue fluorescence intensity (nuclei) using Image-Pro software (v.4.5, Media Cybernetics, Bethesda, MD, USA).

RESULTS

Localization of ABCC11 in normal breast tissue. The localization of the *ABCC11* protein product in normal breast lobules and terminal ducts was determined by immunochistochemistry. The high level of ABCC11 expression was seen in all 10 specimens (Fig. 1, 1N-10N). As shown in Fig. 1-3N, the ABCC11 protein was detected within the layer of both luminal epithelial (Fig.1-3N, hollow arrow) and basal myoepithelial cells (Fig. 1-3N, solid arrow). Of note, normal mammary cells appear to express ABCC11 regardless of the rs178829931 genotype or ER status.

Expression of ABCC11 mRNA. We compared *ABCC11* transcript levels in normal breast tissues and in tumors. As shown in Fig. 2, the increased *ABCC11* expression in cancerous tissue was seen in 4 of 10 patients (Patients 1, 6, 7, and 10). In six patients, the decreased expression as compared to normal breast was observed. The changes in *ABCC11* expression

were irrelevant to the tumor ER status (the obtained ER staining results perfectly corresponded to those in patients' medical records in all cases) or 538G > A (rs178829931) polymorphism. Moreover, no correlation was found between *ABCC11* and *ESR1* expression in tumors (Pearson's correlation coefficient, $r = 0.175$) or in normal breast tissue ($r = -0.182$).

Expression of ABCC11 in BC. IHC analysis revealed an evident decrease in ABCC11 expression in tumor tissues in 8 patients as compared to the normal counterpart (Fig. 1, 1C–5C, 7C, 9C, and 10C). The quantification of green fluorescence intensity revealed 1.8- to 6.7-fold decrease of the signal (Fig. 3). ABCC11 levels in the remaining two BC samples were comparable to those in normal tissue (Fig. 1, 6C, 8C), 1.17- to 1.39-fold signal fading (see Fig. 3). Thus, none of examined tumor samples showed ABCC11 over-expression as compared to normal breast. Interestingly, in three BC samples a very low protein expression was detected despite the high mRNA levels (Fig. 1, 1C, 9C, and 10C).

DISCUSSION

In the present study we found a predominant decrease of the *ABCC11* product, ABCC11 protein, expression in BC as compared to the normal breast tissue of the same patient, and such decrease did not correlate with *ABCC11* mRNA level. Only two of ten BC specimens displayed ABCC11 expression similar to that in the normal tissue.

The function of ABCC-subfamily transporters and their role in tumor resistance are intensively investigated. *ABCC11* mRNA expression data are also available from rather numerous BC analyses. Several studies reported *ABCC11* mRNA over-expression in BC tissue and BC cell lines [8–9, 19–20]. Park *et al.* [19] observed the increased expression of *ABCC11* in BC patients with residual disease compared to those who achieved a complete response, although the authors did not include *ABCC11* in their optimal molecular prognosticator of BC response to neoadjuvant chemotherapy. Honorat *et al.* [10] pointed at the possibility of estrogen involvement in the regulation of *ABCC11* expression. On the other hand, estrogen-responsive genes have been implicated in acquired resistance to tamoxifen or aromatase inhibitors [21]. Taken together, the existing knowledge on ABCC11 expression in BC indicates that this protein may play a role in the regulation of chemotherapy response.

Most studies of tumor resistance are performed using cell cultures. However, the origin of cells used to establish cell lines does not represent all tumor types and the conditions of cell culturing appear to limit translational application of the results obtained in cell lines. Our results show that in a real tissue, *ABCC11* mRNA level poorly correlates with protein expression. This finding emphasizes the importance of parallel examination of *ABCC11* mRNA and protein product in normal and malignant breast tissue. As we demonstrated, surgical samples stored as FFPE tissues could be successfully used for such an analysis.

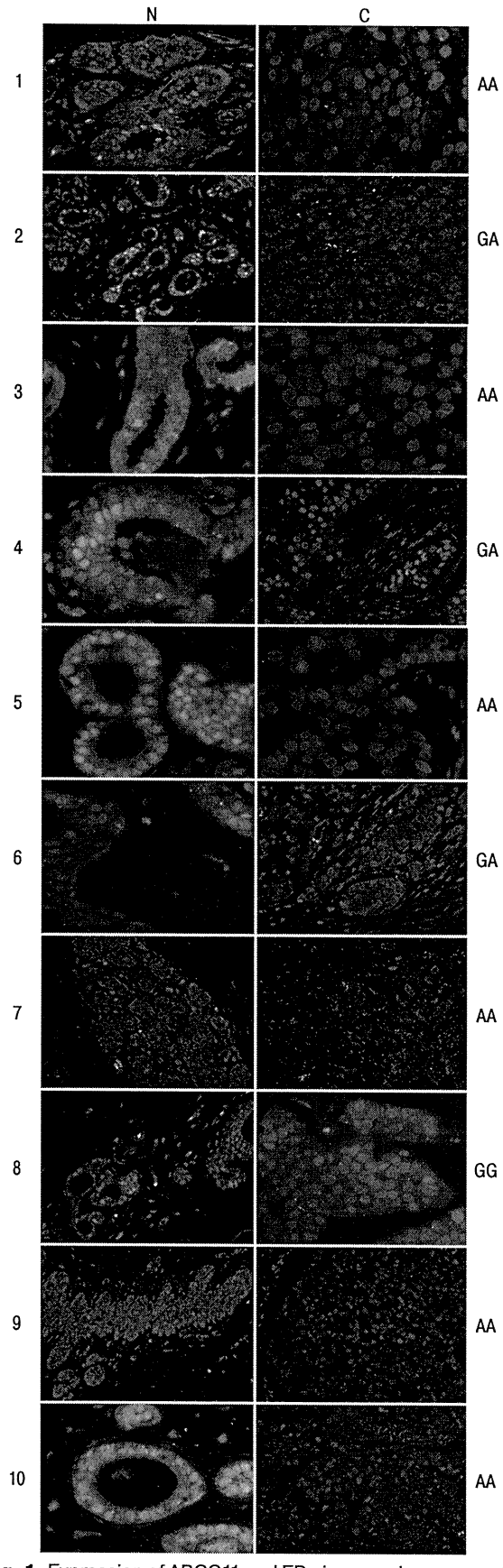

Fig. 1. Expression of ABCC11 and ERα in normal mammary (N, left column) and breast cancer (C, right column) tissues of 10 patients. The ABCC11 protein (green) and the ESR1 protein (red) were detected on 5 μm FFPE sections and merged as described in Materials and Methods. The DAPI counterstaining of the nuclei appears in blue. The genotype at rs17822931 of each patient is indicated on the right of each normal-cancer image pair

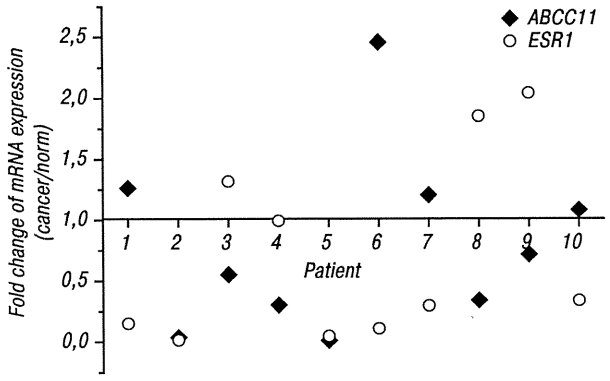

Fig. 2. Expression of *ABCC11* and *ESR1* transcripts in normal mammary tissue and breast cancer tissue of 10 patients. Expression was measured by qRT-PCR, and the geometrical mean of *ABCC11* and *ESR1* relative concentrations against three reference genes was used as an estimate of gene expression level. Black diamonds represent the ratio of *ABCC11* mRNA expression level in BC to that in normal tissue. Circles represent the changes in *ESR1* mRNA expression

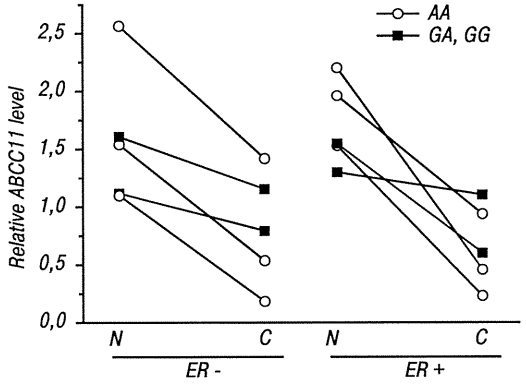

Fig. 3. Down-regulation of ABCC11 protein in BC tissues. The relative intensity of green signal was determined in normal and malignant tissue images as described in Materials and Methods. The decrease of ABCC11 fluorescence intensity from normal (N) to cancer (C) tissue was observed in each patient irrespectively of ER status or genotype

To better understand the role of ABCC11 in BC, the knowledge of protein localization in normal mammary gland is essential. Our experiments employing immunohistochemical staining demonstrated that ABCC11 is expressed in epithelial and myoepithelial cells of breast lobules and ducts. The presence of ABCC11 in epithelial cells of normal terminal duct lobular unit (TDLU), the structural and functional unit of the breast, implies the involvement of this transporter in secretion function of the mammary gland, and is consistent with the finding that the volume of colostrum secretion depends on *ABCC11* genotype at rs17822931 [12]. Of interest is the observation that ABCC11 is expressed also in myoepithelial cells which do not express ERα [22]. Our examination of ABCC11 localization may suggest that the protein participates not only in apocrine secretion, but also in metabolite transport into the stroma embedding ducts and lobules.

Transport activity of ABCC11 is strongly affected by a SNP at nucleotide 538 (538G > A, rs17822931) of *ABCC11* [14]. This SNP determines human earwax type, and associates with some functions of apocrine glands. Individuals with the AA genotype are characterized by the reduced cerumenous secretion [14] and a nearly complete loss of axillary odor [11] as compared to those homozygous or heterozygous for wild-type G allele. However, as the results reported here reveal, the *ABCC11* polymorphism does not seem to influence the localization of the ABCC11 protein in the mammary gland. The ABCC11 expression pattern was similar in the mammary glands of different *ABCC11* genotype carriers, suggesting that non-functional ABCC11 is not degraded but incorporated into the cellular membrane. Similar observations were previously made in the sweat glands [11]. Although ABCC11 expression in normal breast or BC is independent of rs17822931, functional studies of the *ABCC11* SNP are potentially useful. This could be illustrated by the study of the ABCC11 role in lung cancer cell resistance to MTA, in which ABCC11 expression level did not correlate with IC_{50} for MTA; yet *ABCC11* genotype affected chemosensitivity [6].

In conclusion, the expression of ABCC11 protein which localizes in epithelial and myoepithelial cells of normal breast lobules and ducts is likely to be decreased in the majority of BC or it may be comparable to that in normal tissue in some cases. It remains to be elucidated whether ABCC11 loss or retention in BC is functionally relevant to tumor development or may affect clinical course and prognosis. Therefore, further studies of ABCC11 expression in BC are warranted to determine its usefulness for decision making on BC therapy protocol.

ACKNOWLEDGEMENTS

We are grateful to Dr. Vladimir Saenko, Nagasaki University, for his valuable and critical comments. This study was supported by Grant-in-Aid for Science Research (Category B) for N. Niikawa from the Ministry of Education, Culture, Sports, Science and technology of Japan and Research fund in Health Sciences University of Hokkaido.

REFERENCES

1. **Sarkadi B, Muller M, Hollo Z.** The multidrug transporters-proteins of an ancient immune system. Immunol Lett 1996; **54**: 215–9.

2. **Dean M.** ABC transporters, drug resistance, and cancer stem cells. J Mammary Gland Biol Neoplasia 2009; **14**: 3–9.

3. **Chen ZS, Guo Y, Belinsky MG, *et al.*** Transport of bile acids, sulfated steroids, estradiol 17-beta-D-glucuronide, and leukotriene C4 by human multidrug resistance protein 8 (ABCC11). Mol Pharmacol 2005; **67**: 545–57.

4. **Guo Y, Kotova E, Chen ZS, *et al.*** MRP8, ATP-binding cassette C11 (ABCC11), is a cyclic nucleotide efflux pump and a resistance factor for fluoropyrimidines 2',3'-dideoxycytidine and 9'-(2'-phosphonylmethoxyethyl)adenine. J Biol Chem 2003; **278**: 29509–14.

5. **Oguri T, Bessho Y, Achiwa H, *et al.*** MRP8/ABCC11 directly confers resistance to 5-fluorouracil. Mol Cancer Ther 2007; **6**: 122–7.

6. **Uemura T, Oguri T, Ozasa H, *et al.*** ABCC11/MRP8 confers pemetrexed resistance in lung cancer. Cancer Sci 2010; **101**: 2404–10.

7. **Burger H, Foekens JA, Look MP, *et al.*** RNA expression of breast cancer resistance protein, lung resistance-related protein, multidrug resistance-associated proteins 1 and 2, and multidrug resistance gene 1 in breast cancer: correlation with chemotherapeutic response. Clin Cancer Res 2003; **9**: 827–36.

8. **Bera TK, Lee S, Salvatore G, *et al.*** MRP8, a new member of ABC transporter superfamily, identified by EST database

mining and gene prediction program, is highly expressed in breast cancer. Mol Med 2001; **7**: 509–16.

9. **Szakacs G, Annereau JP, Lababidi S, *et al.*** Predicting drug sensitivity and resistance: profiling ABC transporter genes in cancer cells. Cancer Cell 2004; **6**: 129–37.

10. **Honorat M, Mesnier A, Vendrell J, *et al.*** ABCC11 expression is regulated by estrogen in MCF7 cells, correlated with estrogen receptor alpha expression in postmenopausal breast tumors and overexpressed in tamoxifen-resistant breast cancer cells. Endocr Relat Cancer 2008; **15**: 125–38.

11. **Martin A, Saathoff M, Kuhn F, *et al.*** A functional ABCC11 allele is essential in the biochemical formation of human axillary odor. J Invest Dermatol 2010; **130** (2): 529–40.

12. **Miura K, Yoshiura K, Miura S, *et al.*** A strong association between human earwax-type and apocrine colostrum secretion from the mammary gland. Hum Genet 2007; **121**: 631–3.

13. **Nakano M, Miwa N, Hirano A, *et al.*** A strong association of axillary osmidrosis with the wet earwax type determined by genotyping of the ABCC11 gene. BMC Genet 2009; **10**: 42.

14. **Yoshiura K, Kinoshita A, Ishida T, *et al.*** A SNP in the ABCC11 gene is the determinant of human earwax type. Nat Genet 2006; **38**: 324–30.

15. **Consortium TSSHS.** Japanese map of the earwax gene frequency: a nationwide collaborative study by Super Science High School Consortium. J Hum Genet 2009; **54**: 499–503.

16. **Drury S, Anderson H, Dowsett M.** Selection of REFERENCE genes for normalization of qRT-PCR data derived from FFPE breast tumors. Diagn Mol Pathol 2009; **18**: 103–7.

17. **Penland SK, Keku TO, Torrice C, *et al.*** RNA expression analysis of formalin-fixed paraffin-embedded tumors. Lab Invest 2007; **87**: 383–91.

18. **Bustin SA, Benes V, Garson JA, *et al.*** The MIQE guidelines: minimum information for publication of quantitative real-time PCR experiments. Clin Chem 2009; **55**: 611–22.

19. **Park S, Shimizu C, Shimoyama T, *et al.*** Gene expression profiling of ATP-binding cassette (ABC) transporters as a predictor of the pathologic response to neoadjuvant chemotherapy in breast cancer patients. Breast Cancer Res Treat 2006; **99**: 9–17.

20. **Tammur J, Prades C, Arnould I, *et al.*** Two new genes from the human ATP-binding cassette transporter superfamily, ABCC11 and ABCC12, tandemly duplicated on chromosome 16q12. Gene 2001; **273**: 89–96.

21. **Masri S, Phung S, Wang X, *et al.*** Genome-wide analysis of aromatase inhibitor-resistant, tamoxifen-resistant, and long-term estrogen-deprived cells reveals a role for estrogen receptor. Cancer Res 2008; **68**: 4910–8.

22. **Russo J, Ao X, Grill C, *et al.*** Pattern of distribution of cells positive for estrogen receptor alpha and progesterone receptor in relation to proliferating cells in the mammary gland. Breast Cancer Res Treat 1999; **53**: 217–27.

nature genetics

Mutations affecting components of the SWI/SNF complex cause Coffin-Siris syndrome

Yoshinori Tsurusaki[1], Nobuhiko Okamoto[2], Hirofumi Ohashi[3], Tomoki Kosho[4], Yoko Imai[5], Yumiko Hibi-Ko[5], Tadashi Kaname[6], Kenji Naritomi[6], Hiroshi Kawame[7,8], Keiko Wakui[4], Yoshimitsu Fukushima[4], Tomomi Homma[9], Mitsuhiro Kato[10], Yoko Hiraki[11], Takanori Yamagata[12], Shoji Yano[13], Seiji Mizuno[14], Satoru Sakazume[15], Takuma Ishii[15,16], Toshiro Nagai[15], Masaaki Shiina[17], Kazuhiro Ogata[17], Tohru Ohta[18], Norio Niikawa[18], Satoko Miyatake[1], Ippei Okada[1], Takeshi Mizuguchi[1], Hiroshi Doi[1], Hirotomo Saitsu[1], Noriko Miyake[1] & Naomichi Matsumoto[1]

By exome sequencing, we found *de novo SMARCB1* mutations in two of five individuals with typical Coffin-Siris syndrome (CSS), a rare autosomal dominant anomaly syndrome. As *SMARCB1* encodes a subunit of the SWItch/Sucrose NonFermenting (SWI/SNF) complex, we screened 15 other genes encoding subunits of this complex in 23 individuals with CSS. Twenty affected individuals (87%) each had a germline mutation in one of six SWI/SNF subunit genes, including *SMARCB1*, *SMARCA4*, *SMARCA2*, *SMARCE1*, *ARID1A* and *ARID1B*.

Chromatin remodeling factors regulate the gene accessibility and expression by dynamic alteration of chromatin structure. SWI/SNF complexes have important roles in lineage specification, maintenance of stem cell pluripotency and tumorigenesis[1–5]. These complexes are composed of evolutionarily conserved core subunits and variant subunits. Brahma-associated factor (BAF) and Polybromo BAF (PBAF) complexes constitute two major subclasses[1–5]. It has been suggested that the BAF complex is similar to the yeast SWI/SNF complex and that the PBAF complex is more like the chromatin remodelling complex (RSC) in yeast, which is required for cell cycle progression through mitosis[6]. However, several subunits that are common to both BAF and PBAF complexes are predicted to be related to the regulation of lineage- and tissue-specific gene expression[2].

Coffin-Siris syndrome (MIM 135900) is a rare congenital anomaly syndrome characterized by growth deficiency, intellectual disability, microcephaly, coarse facial features and hypoplastic nail of the fifth finger and/or toe (**Fig. 1** and **Supplementary Table 1**)[7]. The majority of affected individuals represent sporadic cases, which is compatible with an autosomal dominant inheritance mechanism. The genetic cause for this syndrome has not been elucidated.

To identify the genetic basis of CSS, we performed whole-exome sequencing of five typical affected individuals (**Supplementary Methods**). Taking into account our model that assumes that an abnormality in a causal gene would be shared in two or more subjects, 51 variants were identified as candidates (**Supplementary Table 2**). All the variants were also examined by Sanger sequencing of PCR products amplified using genomic DNA from the five affected individuals and their parents. Nine variants were found to be false positives, 40 were inherited from either the father or mother, and 2 *de novo* heterozygous mutations of *SMARCB1* were found in 2 affected individuals (c.1130G>A (p.Arg377His) and c.1091_1093del AGA (p.Lys364del)) (**Table 1**, **Supplementary Fig. 1** and **Supplementary Methods**). Two *de novo* coding-sequence mutations occurring within a specific gene is an extremely unlikely event[8], supporting the idea that *SMARCB1* is a causative gene in CSS. Next, we screened *SMARCB1* in 23 individuals with CSS by high-resolution melting analysis[9] and identified the mutation encoding the p.Lys364del alteration in two additional individuals, including one of Arab descent (subject 22) (**Table 1** and **Supplementary Fig. 1**). As the mutation detection rate was relatively low (4 of 23, only 17.4%), we screened 15 additional genes encoding other SWI/SNF subunits (**Supplementary Table 3**). Unexpectedly, four other subunits, *SMARCA4* (also known as *BRG1*), *SMARCE1*, *ARID1A* and *ARID1B* were also found to be mutated (**Table 1** and **Supplementary Figs. 2–5**). In subject 10, a, c.2144C>T mutation in *ARID1B* (encoding p.Pro715Leu) was found in addition to the c.5632delG mutation in *ARID1B*. RT-PCR products that were amplified from total RNA from this subject's lymphoblastoid cells were cloned into the pCR4-TOPO vector. The two mutations were present on different alleles, according to sequencing of clones containing each allele (data not shown). As the c.5632delG mutation is

[1]Department of Human Genetics, Yokohama City University Graduate School of Medicine, Yokohama, Japan. [2]Division of Medical Genetics, Osaka Medical Center and Research Institute for Maternal and Child Health, Izumi, Japan. [3]Division of Medical Genetics, Saitama Children's Medical Center, Iwatsuki, Japan. [4]Department of Medical Genetics, Shinshu University School of Medicine, Matsumoto, Japan. [5]Division of Pediatrics, Japanese Red Cross Medical Center, Tokyo, Japan. [6]Department of Medical Genetics, University of the Ryukyus Faculty of Medicine, Okinawa, Japan. [7]Department of Genetic Counseling, Graduate School of Humanities and Sciences, Ochanomizu University, Tokyo, Japan. [8]Division of Medical Genetics, Nagano Children's Hospital, Azumino, Japan. [9]Division of Pediatrics, Yamagata Prefectural and Sakata Municipal Hospital Organization, Nihonkai General Hospital, Sakata, Japan. [10]Department of Pediatrics, Yamagata University Faculty of Medicine, Yamagata, Japan. [11]Hiroshima Municipal Center for Child Health and Development, Hiroshima, Japan. [12]Department of Pediatrics, Jichi Medical University, Tochigi, Japan. [13]Genetics Division, Department of Pediatrics, Los Angeles County and University of Southern California Medical Center, Keck School of Medicine, University of Southern California, Los Angeles, California, USA. [14]Department of Pediatrics, Central Hospital, Aichi Human Service Center, Kasugai, Japan. [15]Department of Pediatrics, Koshigaya Hospital, Dokkyo University School of Medicine, Koshigaya, Japan. [16]Nakagawa-No-Sato, Hospital for the Disabled, Saitama, Japan. [17]Department of Biochemistry, Yokohama City University Graduate School of Medicine, Yokohama, Japan. [18]Research Institute of Personalized Health Sciences, Health Sciences University of Hokkaido, Ishikari-Tobetsu, Japan. Correspondence should be addressed to N. Matsumoto (naomat@yokohama-cu.ac.jp) or N. Miyake (nmiyake@yokohama-cu.ac.jp).

Received 29 September 2011; accepted 10 February 2012; published online 18 March 2012; doi:10.1038/ng.2219

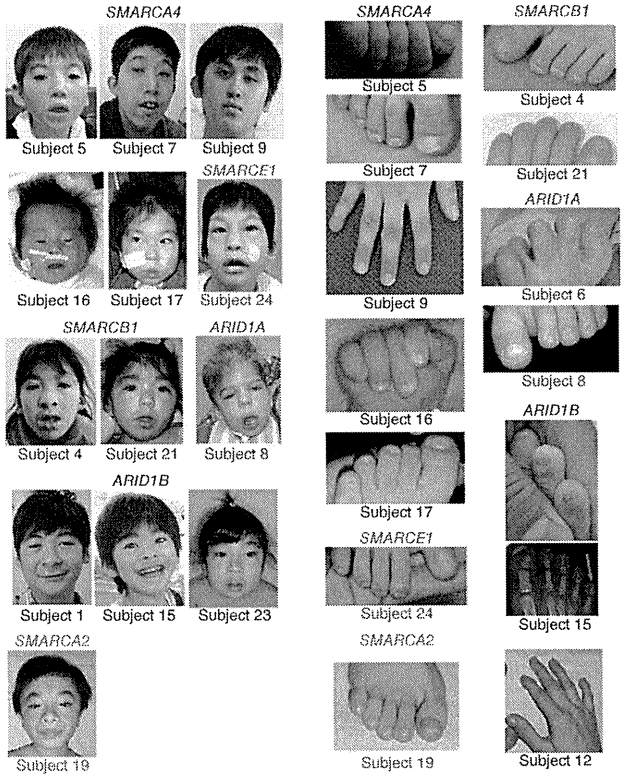

Figure 1 Photographs of individuals with Coffin-Siris syndrome. The faces (left) and hypoplastic-to-absent nail of the fifth finger or toe (right) of affected individuals are shown with the color-coded names of the corresponding mutated genes. The green arrow indicates the absence of the distal phalanx in the fifth toe. No obvious hypoplastic nails were observed in subjects 12 or 19. Consent for all the photographs was obtained from the families of the affected individuals.

very likely to be deleterious (as it results in a truncated protein), the c.2144C>T mutation is likely to be a rare polymorphism. Of note, subject 12, who presented an atypical facial appearance and indistinct hypoplastic nails, had two interstitial deletions at 6q25.3–q27 involving *ARID1B*, as detected by a SNP array (**Supplementary Fig. 6** and **Supplementary Methods**). Furthermore, subject 14 was found to have an interstitial deletion of *SMARCA2* by a SNP array (**Supplementary Fig. 7** and **Supplementary Methods**). No other copy-number changes involving genes encoding SWI/SNF complex components were found in subjects 2, 14 or 18 by array analysis. The overall mutation detection rate was 87%. In total, 20 of the 23 subjects had a mutation affecting one of the six SWI/SNF subunits.

Mutations in CSS were identified in the BAF-specific subunits *ARID1A* and *ARID1B* but not in PBAF-specific subunits (*BRD7*, *ARID2* and *PBRM1*) (**Supplementary Table 3**). In addition, mutations were identified in *SMARCA4* (*BRG1*) as well as in *SMARCA2* (*BRM*) (**Supplementary Table 3**). The BRG1 and BRM proteins are mutually exclusive catalytic ATP subunits in mammalian SWI/SNF complexes. Of note, the majority of heterozygous *Smarca4*-null mice survive with susceptibility to neoplasia, with a minority dying after birth because of exencephaly, whereas homozygous *Smarca2*-null mice are viable and fertile[4]. In *Smarca2*-null mice, Brg1 is upregulated, suggesting that Brg1 can functionally replace Brm in mice[10]. However, in humans, abnormalities in both *SMARCA4* and *SMARCA2* are found in CSS, indicating that the in-frame partial deletion of the gene encoding BRM in subject 19 has a specific mutational effect different from that of simple inactivation in mice. These data support the idea that abnormalities in the BRG1-BAF and BRM-BAF complexes can cause the abnormal neurological development in CSS.

All the mutated genes found in CSS, except for *SMARCE1*, have been reported to be associated with tumorigenesis[1,2]. Among the 23 subjects with CSS, only subject 3 with an *ARID1A* mutation presented with hepatoblastoma. To our knowledge, haploinsufficiency and/or homozygous inactivation of *ARID1A* have been found in several types of cancer but not in hepatoblastoma. Malignancies were not detected in any of the other subjects with CSS examined here. It remains to be seen whether malignancies are robustly associated with CSS.

Given the fact that all the mutations in *ARID1A* and *ARID1B* in CSS were predicted to cause protein truncation, we proposed that haploinsufficiency of these two genes must be able to cause CSS. cDNA analysis of lymphoblastoid cell lines from subjects 1, 6 and 23 indicated that the mutated transcripts were subject to nonsense-mediated mRNA decay (**Supplementary Fig. 8**). In subject 10, the *ARID1B* mutation associated with the creation of a premature stop codon in the last exon did not result in nonsense-mediated mRNA decay as expected (**Supplementary Fig. 8**).

In regard to the other mutated genes, germline heterozygous truncation mutations in *SMARCB1* and *SMARCA4* have been reported

Table 1 Mutations in individuals with Coffin-Siris syndrome

Subject ID	Gene	Mutation	Alteration	Type	Control allele frequency[a]
4	*SMARCB1*	c.1091_1093del AGA	p.Lys364del	*De novo*	0/502
11	*SMARCB1*	c.1130G>A	p.Arg377His	*De novo*	0/500
21	*SMARCB1*	c.1091_1093del AGA	p.Lys364del	NC	0/502
22	*SMARCB1*	c.1091_1093del AGA	p.Lys364del	NC	0/502
9	*SMARCA4*	c.1636_1638del AAG	p.Lys546del	*De novo*	0/350
7	*SMARCA4*	c.2576C>T	p.Thr859Met	*De novo*	0/368
5	*SMARCA4*	c.2653C>T	p.Arg885Cys	*De novo*	0/368
16	*SMARCA4*	c.2761C>T	p.Leu921Phe	*De novo*	0/368
25	*SMARCA4*	c.3032T>C	p.Met1011Thr	NC	0/372
17	*SMARCA4*	c.3469C>G	p.Arg1157Gly	*De novo*	0/368
19	*SMARCA2*	Partial deletion		*De novo*	–
24	*SMARCE1*	c.218A>G	p.Tyr73Cys	*De novo*	0/368
3	*ARID1A*	c.31_56del	p.Ser11Alafs*91	NC	0/330
6	*ARID1A*	c.2758C>T	p.Gln920*	NC	0/376
8	*ARID1A*	c.4003C>T	p.Arg1335*	*De novo*	–
1	*ARID1B*	c.1678_1688del	p.Ile560Glyfs*89	*De novo*	–
15	*ARID1B*	c.1903C>T	p.Gln635*	*De novo*	–
23	*ARID1B*	c.3304C>T	p.Arg1102*	*De novo*	–
10	*ARID1B*	c.2144C>T	p.Pro715Leu	NC	0/368
10	*ARID1B*	c.5632del G	p.Asp1878Metfs*96	NC	0/374
12	*ARID1B*	Microdeletion		NC	–

NC, not confirmed because parental samples were unavailable.
[a]The numbers indicate the observed allele frequency (alleles harboring the change/total tested alleles) in Japanese controls. None of the mutations was found in dbSNP132, the 1000 Genomes database or the National Heart, Lung, and Blood Institute (NHLBI) GO exomesequencing project database. –, not tested.

in individuals with rhabdoid tumor predisposition syndromes 1 (RTPS1; MIM 609322) and 2 (RTPS2; MIM 613325)[11,12], and various types of *SMARCB1* mutations (missense, in-frame deletion, nonsense and splice site) have been found in the germline of individuals with familial and sporadic schwannomatosis (MIM 162091)[13,14]. Furthermore, mice with heterozygous knockout of *Smarca4* or *Smarcb1* were prone to tumor development[2]. All the mutations in *SMARCA4* and *SMARCB1* in individuals with CSS were nontruncating (either missense or in-frame deletions), implying that they exert gain-of-function or dominant-negative effects (excluding haploinsufficiency as a cause). It is noteworthy that comparable germline mutations in *SMARCB1* have such different phenotypic consequences in their association with the phenotypes of CSS and schwannomatosis. The *SMARCB1* mutations in CSS and those in schwannomatosis are indeed different according to the Human Gene Mutation Database. With regard to the *SMARCA2* interstitial deletion in CSS, the change maintained the coding sequence reading frame but removed exons 20–27 that encode the HELICc domain. RT-PCR analysis confirmed the deletion of exons 20–27 at the cDNA level (**Supplementary Fig. 7**). These data suggest the importance of the HELICc domain in the SMARCA2 protein.

The various types of mutations in the genes encoding different SWI/SNF components resulted in similar CSS phenotypes. This suggests that the SWI/SNF complexes coordinately regulate chromatin structure and gene expression. This is the first report, to our knowledge, of germline mutations in SWI/SNF complex genes associated with a multiple congenital anomaly syndrome, highlighting new biological aspects of SWI/SNF complexes in humans. Similarly, genes encoding SNF2-related proteins, which are implicated as chromatin remodeling factors outside of SWI/SNF complexes, are mutated in different syndromes, including in α-thalassaemia/mental retardation syndrome X-linked (ATRX; *ATRX* mutations) and in coloboma, heart defect, atresia choanae, retarded growth and development, genital abnormality and ear abnormality (CHARGE) syndrome (*CHD7* haploinsufficiency)[3]. We expect that more mutations affecting chromatin remodeling factors will be found in different human diseases.

URLs. Human Gene Mutation Database, https://portal.biobase-international.com/cgi-bin/portal/login.cgi.

Note: Supplementary information is available on the Nature Genetics website.

ACKNOWLEDGMENTS

We thank all the family members for participating in this study. This work was supported by research grants from the Ministry of Health, Labour and Welfare (to N. Miyake, H.S. and N. Matsumoto), the Japan Science and Technology Agency (to N. Matsumoto), the Strategic Research Program for Brain Sciences (to N. Matsumoto), the Japan Epilepsy Research Foundation (to H.S.) and the Takeda Science Foundation (to N. Matsumoto and N. Miyake). This study was also funded by a Grant-in-Aid for Scientific Research on Innovative Areas (Foundation of Synapse and Neurocircuit Pathology) from the Ministry of Education, Culture, Sports, Science and Technology of Japan (to N. Matsumoto), a Grant-in-Aid for Scientific Research from the Japan Society for the Promotion of Science (to N. Matsumoto), a Grant-in-Aid for Young Scientists from the Japan Society for the Promotion of Science (to N. Miyake and H.S.) and a Grant for 2011 Strategic Research Promotion of Yokohama City University (to N. Matsumoto). This study was performed at the Advanced Medical Research Center at Yokohama City University. Informed consent was obtained from all the families of affected individuals. The Institutional Review Board of Yokohama City University approved this study.

AUTHOR CONTRIBUTIONS

Y.T., S. Miyatake, I.O., H.D., H.S. and N. Miyake performed exome sequencing and Sanger sequencing. Y.T., M.S., K.O., I.O., T.M., H.D., H.S. and N. Miyake performed data management and analysis. N.O., H.O., T. Kosho, Y.I., Y.H.-K., T. Kaname, K.N., H.K., K.W., Y.F., T.H., M.K., Y.H., T.Y., S.Y., S. Mizuno, S.S., T.I., T.N., T.O. and N.N. provided clinical materials after careful evaluation. Y.T., N. Miyake and N. Matsumoto wrote the manuscript. N. Matsumoto designed and oversaw all aspects of the study.

COMPETING FINANCIAL INTERESTS

The authors declare no competing financial interests.

Published online at http://www.nature.com/naturegenetics/.
Reprints and permissions information is available online at http://www.nature.com/reprints/index.html.

1. Reisman, D., Glaros, S. & Thompson, E.A. *Oncogene* **28**, 1653–1668 (2009).
2. Wilson, B.G. & Roberts, C.W. *Nat. Rev. Cancer* **11**, 481–492 (2011).
3. Clapier, C.R. & Cairns, B.R. *Annu. Rev. Biochem.* **78**, 273–304 (2009).
4. Bultman, S. *et al. Mol. Cell* **6**, 1287–1295 (2000).
5. Hargreaves, D.C. & Crabtree, G.R. *Cell Res.* **21**, 396–420 (2011).
6. Xue, Y. *et al. Proc. Natl. Acad. Sci. USA* **97**, 13015–13020 (2000).
7. Coffin, G.S. & Siris, E. *Am. J. Dis. Child.* **119**, 433–439 (1970).
8. Bamshad, M.J. *et al. Nat. Rev. Genet.* **12**, 745–755 (2011).
9. Wittwer, C.T., Reed, G.H., Gundry, C.N., Vandersteen, J.G. & Pryor, R.J. *Clin. Chem.* **49**, 853–860 (2003).
10. Reyes, J.C. *et al. EMBO J.* **17**, 6979–6991 (1998).
11. Schneppenheim, R. *et al. Am. J. Hum. Genet.* **86**, 279–284 (2010).
12. Taylor, M.D. *et al. Am. J. Hum. Genet.* **66**, 1403–1406 (2000).
13. Boyd, C. *et al. Clin. Genet.* **74**, 358–366 (2008).
14. Hadfield, K.D. *et al. J. Med. Genet.* **45**, 332–339 (2008).